Appl. Phys. B 79, 871–877 (2004)
DOI: 10.1007/s00340-004-1647-7

Applied Physics B
Lasers and Optics

L. HOLMLID

Detection of frequency red shifts and blue shifts for single-mode IR laser radiation in Rydberg matter

Atmospheric Science, Department of Chemistry, Göteborg University, 412 96 Göteborg, Sweden

Received: 19 May 2004/Revised version: 19 August 2004
Published online: 29 September 2004 •

ABSTRACT Stimulated emission and laser gain were recently reported for the excited condensed matter Rydberg matter (RM). This shows that RM is in an excited and inverted state. A low-intensity single-mode IR laser beam is here red shifted in reflection from a layer of RM, and blue shifted when it passes through a cloud of RM. The shifts of approximately 0.02 cm^{-1} are observed with a temperature-stable Fabry–Pérot interferometer. The process giving the wavelength shifts is proposed to be stimulated Raman scattering. RM is here formed from Rydberg states of both K atoms and nitrogen molecules inside a vacuum chamber, and it may be in liquid or solid form.

PACS 78.30.-j; 42.65.Dr; 42.55.Ye

1 Introduction

Stimulated emission was recently studied using the electronically excited condensed phase Rydberg matter (RM) as the active medium [1, 2] in a laser cavity. Research in this field is thus needed to focus on the electronic degrees of freedom; the structure of RM is now quite well studied, with recent results on the $n = 1$ excitation state [3]. Further, recent studies of the liquid and solid properties of RM [4] and of its relation to cold Rydberg gases and plasmas [5] give a better framework to describe the general properties of RM. An improved understanding of the electronic and bonding properties of RM should be found from a study of the interaction between RM and light in various frequency bands. The propagation of radiation in interstellar and intergalactic space [6] is of interest in this context, and it was recently proposed [7] that stimulated Raman scattering in intergalactic matter gives rise to the quantized red shifts observed. The stimulated Raman study [8] with IR diode-laser beams passing through RM was a starting point for the present project. That investigation revealed both frequency shifts in transmission through the Rydberg matter and interaction between the laser modes passing through the Rydberg matter. Another recent IR study concentrated on the somewhat simpler reflection properties [9]. A model was proposed which describes the interaction between the laser modes in the RM. In the present study, the frequency shifts of IR light in both transmission and reflection from Rydberg matter are studied.

Rydberg matter is a condensed phase formed by condensation of circular, long-lived Rydberg states of atoms and small molecules. The Rydberg electrons interact and give a delocalized metal-like bonding in the matter with a half-filled conduction band. This means for example that it is impossible to observe Rydberg series from the atoms or molecules forming this matter. The structure of RM was predicted by Manykin et al. more than 20 years ago [10, 11], but it was only by 1991 that the first macroscopic experimental studies of this low-density metallic phase were performed [12, 13]. Improved quantum mechanical calculations of the macroscopic properties of RM built up by Cs Rydberg states were also published later [14, 15]. Studies by time-of-flight methods [16] have identified the special planar cluster shapes predicted by theory [17]. Recently, the excitation states and bonding distances in RM formed by hydrogen and nitrogen molecules have been studied with similar techniques [18–21].

The early results from our group on RM have recently been independently confirmed. Results on RM formed from Cs in a plasma environment were reported by Yarygin et al. [22]. Apart from confirmation of the extremely low work function and high conductivity of RM, the authors observed long-lasting visible emission, probably from RM clusters. Such emission is not observed under conditions with only plasma formation. The first step in the formation of RM from an emitter is desorption of RM clusters and other Rydberg species. This step was confirmed in studies by Kotarba et al. [23–25]. They even observed that catalytically active surfaces emit Rydberg species, while similar, catalytically inactive surfaces do not give Rydberg-species formation.

2 Theory

RM is a special liquid or solid (crystal) form of matter; it is the condensed phase formed from interacting circular Rydberg species. Circular Rydberg states are very long-lived due to small overlap with lower electronic states, and the radiative lifetime at principal quantum number $n = 100$ is of the order of 20 s [26]. Condensation to RM implies strong electron correlation [17] and much longer lifetime against spontaneous decay, of the order of Gy at $n = 100$ from an

✉ Fax: +46-31-772-3107, E-mail: holmlid@chem.gu.se

extrapolation of the results in [11]. The interactions (bonding forces) between the Rydberg species are normal chemical (exchange-correlation) forces, and the circular electrons are delocalized in what may be called a conduction band. RM is thus a low-density metal [12, 13] at not too low densities, and can be formed from many atoms and small molecules: the studies so far have mainly used Cs, K, H_2 and N_2. The bonding distances (interionic distances) are quantized, with small n values giving shorter distances and a denser material. These distances can be measured directly by laser fragmentation and Coulomb explosions. The state $n = 1$ that is only possible for hydrogen atoms is the most compact form of RM; it has an interatomic bonding distance of 150 pm as verified in recent experiments [3]. Normally, the excitation state of RM formed in the laboratory is $n = 40$–80. The lifetime of RM under such conditions is minutes (high temperature)–hours (300 K or lower). A factor contributing to these long lifetimes is the self-cooling observed experimentally. RM formed from K atoms has been shown to reach temperatures of < 20 K, probably due to stimulated emission [21].

RM is most easily produced by desorption of alkali atoms from non-metal solid surfaces in high vacuum, at temperatures > 300 K. A quite complete description of the methods used to form RM is given in [27]. The desorbed species are small clusters; when cooled in a vacuum after desorption they take the most stable six-fold symmetric planar form (its solid crystal form) [17]. This means that so-called magic numbers (number of atoms or molecules in the clusters) are found at $N = 7$, 19, 37, 61 and 91. In the present experiments, the clusters form a cloud which is probed by the laser beam, and the cluster structure is of little significance. The exact state (liquid or solid) of the clusters and the cloud is not known, and this state will probably not influence the results strongly. Just a few publications on RM are cited here, but further results are quite easily found in the scientific literature.

An interaction of RM with laser light is possible through stimulated Raman processes. The weak interaction between RM and light otherwise, however, seems to prevent normal absorption and spontaneous emission studies in the laboratory. Stimulated Raman studies of RM have utilized intense pulsed lasers in the visible range [28] and weak cw lasers in the IR range [8]. Stimulated Raman scattering in general is described in an excellent review [29] and in books on non-linear optics [30, 31] and laser spectroscopy [32].

The processes of interest are anti-Stokes stimulated electronic Raman scattering (ASERS) [29] and its Stokes counterpart. The description here will mainly cover the anti-Stokes (blue-shifting) process, but the Stokes (red-shifting) process can be described in similar terms. The upper level from which the energy is depleted and where an inversion relative to the ground state exists is any electronically excited level in the RM, with the ground state corresponding to the lowest level in the RM at the excitation level characterized by the principal quantum number n. Collective effects in the condensed RM phase exist and, at the RM densities used here, the condensed phase consists of interacting planar clusters. The energy difference between the ionization limit and the lowest level in RM at an excitation level of $n = 50$ is 44 cm^{-1} for each Rydberg atom, thus giving energy differences between 310 and 2600 cm^{-1} for cluster sizes $N = 7$–61 [18–21]. This is comparable to the laser photon size used here of approximately 1000 cm^{-1}, and the intermediate state may thus be either a resonant state in the RM or a virtual state above the ionization limit for a small cluster. This is true even if the thermal excitation level above the ground state of the RM would be of the order of $kT \approx 600\,\mathrm{cm}^{-1}$ at 900 K. There is no phase-matching condition for this type of process [29], and the light proceeds in the same direction as the incoming laser light. The incoming laser frequency is ω_L and the anti-Stokes wave is ω_as. The difference $(\omega_\mathrm{as} - \omega_\mathrm{L}) = \omega_\mathrm{E}$ is an electronic excitation in the RM material. The pumping laser beam is attenuated and the anti-Stokes wave is amplified. However, in the present case there is just a small increase in the total energy since the excitations in the RM are small. For the anti-Stokes wave in the steady-state regime which ought to be applicable here, the classical gain factor G_ss is of the same form as the gain factor for Stokes-wave generation at its maximum with $(\omega_\mathrm{as} - \omega_\mathrm{L}) = \omega_\mathrm{E}$ [31]:

$$G_\mathrm{ss} = \frac{N k_\mathrm{as}}{8 m \varepsilon \gamma (\omega_\mathrm{as} - \omega_\mathrm{L})} \left(\frac{\partial \alpha}{\partial q}\right)_0^2 |E_\mathrm{L}|^2 \ . \tag{1}$$

The quantities entering this expression are N, the density of the dipoles created by the incoming laser wave here chosen to correspond to the number of electrons in the RM, k_as, the wave number for the anti-Stokes wave, m, the mass of the driven oscillator, in this case one electron mass, $\varepsilon = \varepsilon_\mathrm{r}\varepsilon_0$, the permittivity of the medium which is unknown but probably has ε_r of the order of unity, γ the coupling constant for the electronic excitation in the intermediate state to other degrees of freedom, $\partial\alpha/\partial q$, the variation of the polarizability with the coordinate describing the excited motion, here the electronic motion, and E_L, the electric field strength of the incoming laser. This expression is valid if $\gamma \ll \omega_\mathrm{E}$.

The reason why this gain factor can be so large in the present case is the very large polarizability of the RM, and the small value of the difference $(\omega_\mathrm{as} - \omega_\mathrm{L}) = \omega_\mathrm{E}$. The reason for this small value is the almost continuous energy levels in RM. The possibility that the intermediate state is a resonance state in RM should also increase the transient absorption in RM. Another factor of great importance is the coupling (dephasing) constant γ, which is much smaller than for ordinary matter since the coupling of the electronic motion in RM to other modes of motion is weak. This will be discussed below.

In [8] the size of the anti-Stokes Raman effect for the passage of light through RM was estimated. The stimulated Raman effect was found to be large. In the present case, RM is formed in a small vacuum chamber. A weak IR laser beam is transmitted through the RM or partially reflected from the inner face of a vacuum window with an RM layer. Since the evanescent wave at the window may extend into the RM deposited on the inner face by more than one wavelength, the sampling depth into the RM phase is at least 10–20 μm in the reflection experiments. An air-spaced Fabry–Pérot interferometer (FPI) is used to observe the wavelength shifts. The signal is studied mainly as a function of the amount of RM formed by heating the RM emitter and the temperature of the window in the vacuum chamber.

Experimental problems like temperature effects on the FPI and drifts in the mode structure of the diode lasers must be

taken into account. This is described below in Sects. 3 and 5. It is apparent that a slow energy decay and/or gain of the photons coupled to the RM structure in the stimulated Raman process exists [8], which means that the excitation decreases or increases in size in time. In [8], the coupling constant γ for the coupling of electronic excitation to other degrees of freedom was determined to be $< 10^2\ s^{-1}$. This coupling constant is not related to the excitation state of RM, i.e. the common principal quantum number giving the interionic distances in the RM structure, but to the excitation of the electrons above the ground state of RM for each excitation state. This type of excitation may be translational excitation of the electrons in the planar clusters which form the RM cloud [7, 17, 19]. The lifetime of the RM in its collectively excited state characterized by a principal quantum number is much longer, from minutes to hours [8, 12, 13, 28].

3 Experimental

A diode-laser spectrometer (MDS 1000 from Mütek, Hersching, Germany) was used for the experiments. It consists of a laser holder with a closed-cycle He cooler (Leybold–Heraeus) going down to < 30 K. The laser used (Laser Components, München, Germany) is a lead-salt laser centered at $1080\ cm^{-1}$ (main range $1060–1200\ cm^{-1}$). The line width of the laser modes for such a laser is of the order of $10^{-4}\ cm^{-1}$. The scan width at each temperature point for the laser is approximately $25\ cm^{-1}$, and the slope of the modes is approximately $7 \times 10^{-3}\ cm^{-1}\ mA^{-1}$. The experimental setup, shown in Fig. 1 for the case of reflection at the inner surface of the window, is similar to the one used in [8] but with a Fabry–Pérot interferometer directly after the vacuum chamber.

In the transmission experiments, the laser beam is focused on the small entrance ZnSe window at an angle of 9° by an off-axis parabolic gold mirror with a focal length of 90 mm. At the other end of the vacuum chamber, a spherical gold mirror is mounted with its radius chosen so that the laser light is focused again on the exit ZnSe window, at a distance of 150 mm. The direct IR emission from the emitter and the RM cloud [20] may reach the detector in this case.

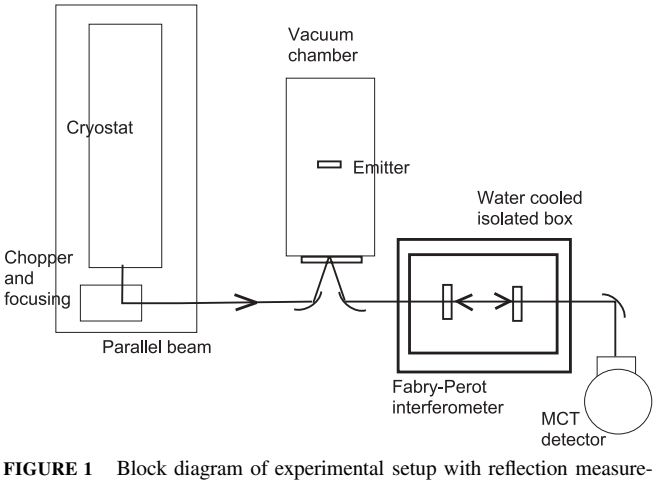

FIGURE 1 Block diagram of experimental setup with reflection measurement, vertical view. The emitter is heated so that RM is formed as a 'cloud' in the vacuum chamber surrounding the emitter, also giving a deposit on the window. For a complete description, see text

In the reflection measurements, the laser beam is focused by the same parabolic entrance mirror on another 2-mm-thick ZnSe window in the chamber wall. This window is antireflection coated for 10.6 μm on the outer (air) surface. The laser beam is reflected from the central 5-mm-diameter part of the window, defined by a metal support for the window in the chamber. The central ray makes an angle of approximately 23° to the window normal, thus decreasing any reflections in the window by shifting such reflected light along the window out of the beam-reflection spot. The direct IR emission from the emitter cannot reach the detector in this case.

The vacuum chamber is pumped by a $200\ l\ s^{-1}$ diffusion pump and air is usually leaked in to a pressure of 1×10^{-4} mbar. RM is in this case formed both from K* Rydberg atoms and N_2^* Rydberg molecules [1, 2, 19–21]. In the chamber at a distance of 40–80 mm from the window, a K-impregnated metal oxide sample that emits RM is mounted. This emitter is in cylindrical form with a diameter of 3 mm. It is wrapped in a tube of Ta foil and heated to a temperature up to 1300 K by 50 Hz ac current. One side of the Ta foil is cut away so that the flux of RM can be emitted out into the chamber or onto the inner face of the window. The emitter is a commercial iron oxide catalyst, impregnated with K at initially 8 wt. %. It is used in the chemical industry for production of styrene from ethyl benzene.

The light beam from the chamber is taken to an off-axis parabolic mirror that gives a parallel beam. This beam is focused once more by an off-axis parabolic mirror onto an MCT (HgCdTe) detector. The signal is detected in-phase and digitized and registered by a PC computer board at an integration time of 100–500 ms. The drive current to the laser diode is swept linearly in time and the detector signal recorded. The temperature of the laser diode is almost constant as set during the current sweep, and there are no slow changes observed during the experiments.

The Fabry–Pérot interferometer (FPI) consists of two 3-mm-thick ZnSe mirrors which are mounted in holders with micrometer adjustments down to 1 arc sec (Melles–Griot). The mirrors (Janos Technology, Townshend, Vermont, USA) have reflectivities at 10.6 μm of 50%–85% on one face. The other surfaces are antireflection coated at the same wavelength. The two mirror holders are mounted on a plate of Invar (NILO alloy 36, linear thermal expansion coefficient $1.5 \times 10^{-6}\ K^{-1}$) at a distance of 26 mm between their inner surfaces. The free spectral range is thus $0.19\ cm^{-1}$ with the highly reflective surfaces facing each other. The Invar plate can be water cooled. The whole interferometer construction with its two fixing magnet feet can be covered by a well-insulated box to improve its temperature stability. The temperature of the FPI Invar plate or of one of the mirror holders is measured with an NTC resistor (10 kΩ at 25 °C). The temperature often increases slightly during the run, typically < 1 K. The cooling water temperature is usually more constant.

In the experiments, the drive current to the laser diode is scanned, increasing linearly in size with time. The shifts of the FPI fringes are observed since the fringe maxima appear at other drive-current values I. The two main effects which influence the position of the fringes are the wavenumber shift $\Delta\tilde{\nu}$ of the laser light due to the stimulated Raman process, and the

temperature effect changing the length of the FPI cavity by an amount Δl. Both these effects can be included in the formula for the drive current I as

$$I = c_1(m/(l + \Delta l) - \Delta\tilde{\nu}) , \quad (2)$$

where m is the number of wavelengths within the cavity length l and c_1 is a parameter describing the (non-continuous) relation between I and $\Delta\tilde{\nu}$.

4 Results

Results from a typical transmission experiment are shown in Fig. 2. The scans are all taken on the same day at an air pressure of 1×10^{-4} mbar in the chamber. During the first part of the experiment the emitter was cold, with relatively little RM in the cloud surrounding it. During a few hours, the RM emitter was heated, giving a denser RM cloud. Finally, the RM cloud cooled itself during one hour or so after the emitter was turned off. The times for the laser scans are given. The status of the emitter is indicated in the figure, together with the temperature of the FPI base.

The FPI fringes shift in the scans. A shift to the left in the plot means that the fringes shift to lower drive current where the frequency emitted from the laser is lower. Thus, this shift shows that the interference condition at the FPI is met with lower laser current, with the light passing the FPI shifted to higher frequencies. This shift is thus a blue shift, while a shift to the right in the plots is a red shift. In Fig. 2, a gradual shift to the blue is observed after heating, and to the red during cooling. Simultaneously with the blue shift, the signal decreased strongly. During the last part of the experiment, the temperature of the FPI was constant, while the light shifted to the red. The temperature of the emitter and chamber walls dropped much faster than the time it took for the blue shift to go over to a red shift. In Fig. 3, three of the scans from Fig. 2 are compared, showing that a red shift is observed for the last scans even relative to the scan taken just before the start of emitter heating. This type of behavior is observed in many experiments each one lasting one day. Thus, this effect is reproducible.

Simultaneously with the blue shift, the signal decreases in amplitude. This may be due to absorption in the RM cloud, as suggested previously [8], but it may also be due to changes in reflection at the inner window surfaces or at the gold mirror in the chamber, where some RM may deposit. As can be seen, this effect is anyway easily reversible within an hour or so, not indicating any low vapor pressure deposits like K metal from the emitter.

Results from a typical reflection experiment are shown in Fig. 4. The signal to the detector is much lower in this case, since a large part of the laser beam is not reflected and thus does not reach the detector. This gives a more noisy signal relative to Fig. 2. With increasing exposure to the RM emit-

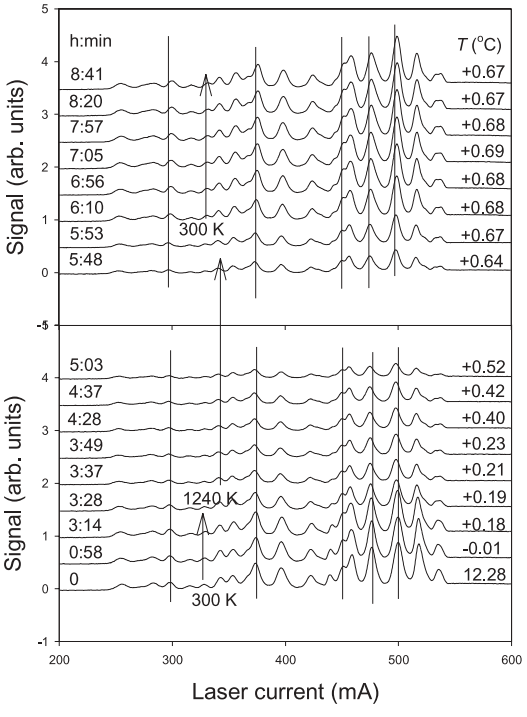

FIGURE 2 A transmission run showing both blue shift (shifting to the *left* in the figure) and red shift as a function of the heating of the RM emitter. Times of the laser scans, the emitter status and the temperature of the FPI base are indicated. Each scan took 5 min, with 1000 measured points

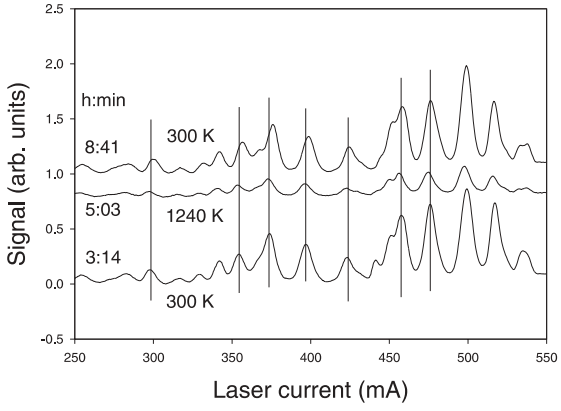

FIGURE 3 The extreme shifted scans from the data in Fig. 2 together with an initial stable unshifted scan

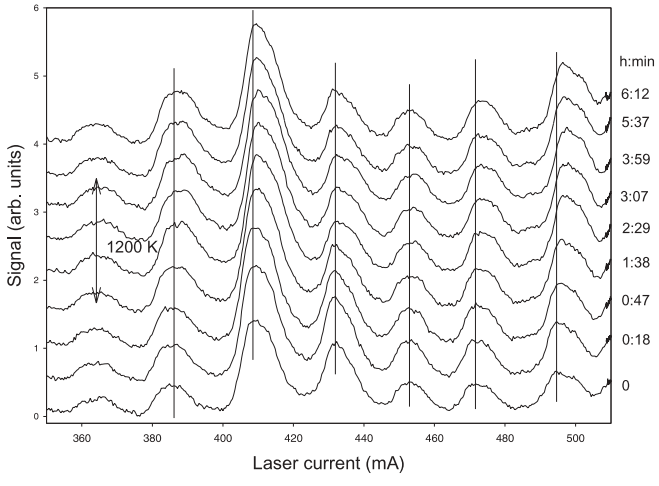

FIGURE 4 A reflection run showing red shift of the fringes at high emitter temperature and afterwards. The temperature of the FPI increased from 20.24 °C to 21.92 °C during the experiment, which should introduce a blue shift

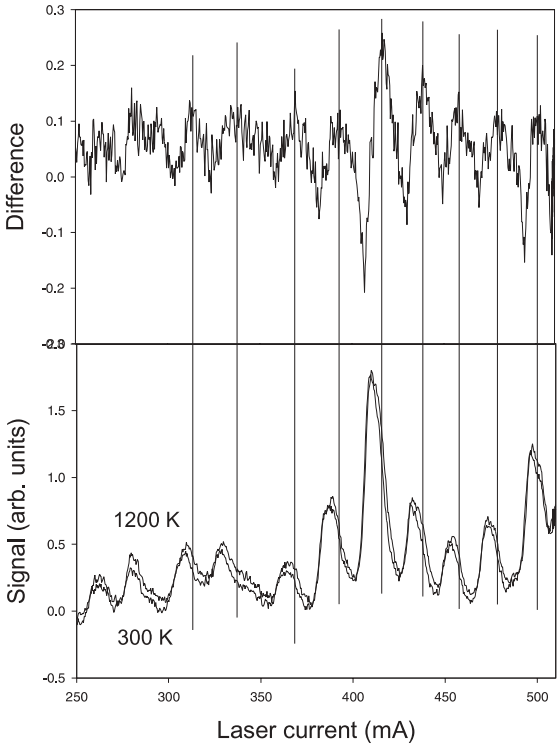

FIGURE 5 Two scans from Fig. 4 (*lower*), with the difference (*upper*). The 300 K curve is the last one measured in Fig. 4 at time 6:12 after the start of the experiment and at a temperature of 21.92 °C, while the 1200 K curve is measured at time 3:59 and at a temperature of 21.69 °C. The maximum signal change at high temperature with RM is at larger laser drive current, thus indicating a red shift

ter flux, the reflected signal becomes red shifted, i.e. shifted to the right in the figure. At the same time, the interference maxima broaden slightly, indicating that the signal becomes less well defined in frequency. This is expected since the quanta in the stimulated Raman process are much smaller than the total shift observed, and since the light beam is reflected non-uniformly over the central area of the window which is partly blocked by the internal supporting structure. In Fig. 5, the red shift of a scan with a hot RM emitter is compared to a scan taken with a cold emitter more than two hours later. Thus, the red shift is reproducible relative to scans taken both before and after the emitter is heated. Similar results have been found with the two scans at identical FPI temperatures. The subtraction of the two scans in the upper panel of the figure shows that the maximum increase of the signal is at higher wavenumbers (drive current) than the actual peak of the FPI fringe. Similar plots are presented in [8] for the case of blue shifting in transmission. Reflection experiments have also been done with an almost entirely closed Ta foil surrounding the RM emitter. In such cases, no red shift is observed.

The observation of both blue shifts and red shifts shows that a symmetry exists of the form expected for anti-Stokes and Stokes stimulated Raman shifts. Another form of such a symmetry is observed in the mode-interaction experiments [9]. The results obtained in reflection may be due to a forward-moving Stokes wave. How such a wave will behave in evanescent-wave mode is not well known. However, a similar setup with stimulated emission from the RM layer with just evanescent-wave interaction worked well [33]. Thus, a reflected Stokes wave is likely to give the red shifting observed.

5 Discussion

5.1 *Temperature changes of the FPI*

Despite the care taken in the construction of the interferometer, a temperature change in the interferometer is of course the main problem with the measurements. The effect of temperature changes of the order of 1 K is very small; see the example in Fig. 2. The absolute value of the temperature coefficient is found to be $< 1.5 \times 10^{-2}\,\mathrm{cm^{-1}\,K^{-1}}$ for setups with a positive coefficient (mirrors facing inwards), and slightly smaller in cases with a negative coefficient (one mirror facing outwards). Direct tests of the temperature effect are often done after the experiments for the special conditions (mounting and adjustment of mirrors in the FPI). The true, directly observed temperature variation is often very small, with a main contribution from the base plate and less from the mirror holders. The base plate of the FPI changes very little in temperature during a typical run. Thus, the effects observed are not due to temperature changes of the interferometer.

The coefficient of thermal expansion α for the construction material in the interferometer base, micrometer screws, etc., gives a shift of the interferometer fringes as $\mathrm{d}\tilde{\nu}/\mathrm{d}T = \alpha\tilde{\nu}$. With typical values of $\alpha = 1 \times 10^{-5}\,\mathrm{K^{-1}}$ and $\tilde{\nu} = 1000\,\mathrm{cm^{-1}}$, the typical temperature effect expected is $10^{-2}\,\mathrm{cm^{-1}\,K^{-1}}$, in good agreement with the observed temperature coefficient. With a spacing of the fringes of $0.19\,\mathrm{cm^{-1}}$, such effects correspond to only a 5% shift, that is $0.01\,\mathrm{cm^{-1}}$ in the fringe peak position for a 1-K temperature change. The shifts observed and reported here are around $0.02\,\mathrm{cm^{-1}}$ for small simultaneous temperature changes, < 0.2 K. Thus, it is concluded that the shifts of the fringes observed are not due to changes in the temperature of the interferometer. In some cases, experiments have been done with setups with both positive and negative coefficients, to remove any uncertainty. Shifts are also observed for a hot relative to a cold RM emitter, even in cases where the FPI temperature is constant.

5.2 *Drifts of the laser modes*

During experiments that lasts for days, drifts and changes in the laser modes are sometimes detected. Such changes are distinguished from the wavelength shifts reported here in the way that they do not happen for all the modes simultaneously, so by studying the full laser range it is possible to conclude what kind of change has taken place. The experiments are also repeated and shown to be reproducible. In practically all cases, the intrinsic changes of the laser modes are observed as step changes after the laser has been turned off for a longer period, like overnight, which is easily observed and avoided as a source of error. Only controlled slow changes of all laser modes simultaneously are taken to show true wavelength shifts simultaneously with changes of the emitter conditions. This is the reason why full sets of results are shown here as in Fig. 2. The red shift in Fig. 5 is in fact observed relative to the last scan measured in Fig. 4. If drift was responsible for this effect, the drift had to change sign at the same time as the heating of the RM emitter was interrupted.

This demonstrates convincingly that the effects observed are not due to intrinsic mode shifts in the laser.

The red shifts and blue shifts are reproducible. They can be observed with the same equipment, just changing the interaction with the RM between reflection and transmission, as shown here. Thus, no systematic error where the IR light from the RM emitter or from the chamber wall influences the temperature of the laser diode can exist.

Other methods to identify the drifts in the laser modes have been tested. For example, by reflecting the laser beam around the vacuum chamber directly to the FPI and detector, one may be able to detect laser mode changes. However, we were not able to make the beam path reproducible enough for the passage outside the chamber to make this method useful; small angular shifts of the mirrors changed the FPI pattern too much. Without the FPI, the mode structure is not observed at all since the intensity of the laser is a smooth function of the drive current. Thus, the FPI is necessary to observe changes in the wavelength. Another possibility might be to use absorption in gas samples as reference points for the diode lasers. With the laser used here, methanol should be useful for calibration, but the bands are too broad to give any precise standard. N_2O would be the most suitable standard judging from the NIST database and may have sharp enough bands. The gas cell must be mounted in the laser beam before the chamber with an otherwise unchanged setup. However, the wavelength broadening of the beam observed due to the stimulated Raman process together with the action of the FPI will probably mask any shifts in the laser during an experiment with heating of the emitter. The evidence from the detection of both red shifts and blue shifts given above is considered stronger than any evidence possible from such a calibration in the experiment.

5.3 *Apparent absorption*

In the transmission experiments the intensity of the laser beam to the detector decreases strongly when RM is formed, as seen in Fig. 2. The reason for this may be absorption in the RM cloud, reflection at the entrance and exit windows due to RM deposition or inhomogeneous broadening of the laser light due to the stimulated Raman process that will give less constructive interference in the FPI.

The decrease of the signal observed in other studies like the transmission study [8] and the reflection study [9] was much smaller. In the reflection study [9], as also observed here, the signal may even increase when RM is formed. In the transmission study [8], it was concluded that a detector non-linearity could not be the reason for the apparent absorption. The same reasoning is valid here, since the use of the FPI would decrease such an effect and since the effect is larger here than in cases without the FPI [8].

The observation that the size of the signal in general and also that the FPI fringes increase at the end of a run also made it possible to discard accumulation of metal layers or similar on the windows and mirrors in the apparatus as the reason for the signal decrease at high emitter temperature [8]. This behavior is also seen in the present experiments, for example in the run in Fig. 2. Since the effect observed now is so large when the FPI is used, it is concluded that the effect is mainly due to wavelength broadening by the stimulated Raman process.

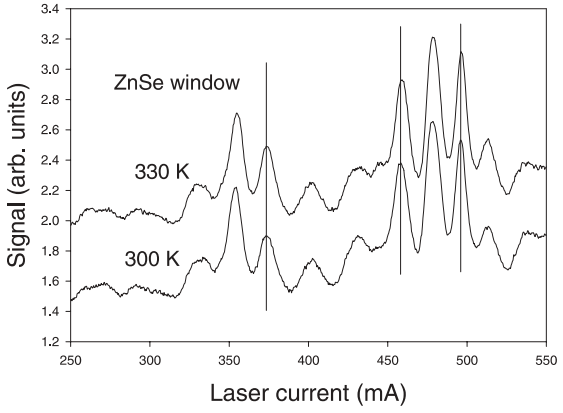

FIGURE 6 An experiment with hot-air heating of the reflecting window in the vacuum chamber. The window heating did not shift the FPI fringes even at a temperature increase of 30 °C. The emitter was at room temperature, and the FPI base at 12.72 °C in both scans

Supporting evidence is found from reflection measurements. When the reflective window is heated to 50 °C by a hot-air fan, the FPI fringes increase in size. A typical case is shown in Fig. 6. If any reflective layer was removed by the heating, the signal would decrease. The change in refractive index and thus in reflectivity by the ZnSe material is $< 2 \times 10^{-3}$, much too small to account for the observed change. It is concluded that this effect is due to removal of a layer on the window that gives broadening of the single-mode laser light, as is the case for RM.

5.4 *Solid or liquid state of RM*

Since the RMs used in the transmission and reflection experiments probably have quite different temperatures, it is relevant to consider possible changes in the state of RM, being solid (crystalline) or liquid. We do not know the exact excitation state of the RM under the conditions of the experiment. However, under conditions similar to the formation of the cloud observed in Fig. 2, we find excitation levels in stimulated emission experiments to be $n = 40$–80 [2]. Due to the rather high pressure used in the present experiments, a very strong self-cooling [21] should not be possible: however, stimulated emission is rapid even under such conditions [2]. We assume thus that a temperature of > 300 K exists in most of the cloud surrounding the emitter in the transmission measurements with a hot emitter. This is probably sufficiently high to give a liquid form of RM, since the bond energy of RM at $n = 40$ is estimated to be only approximately 40 K. With a cold emitter in Fig. 2, a red shift is observed. This could be due to the formation of a cold, maybe partly solid (of course still fractal) cloud at < 300 K around the emitter.

In the reflection experiments, exemplified by Fig. 4, a stronger cooling of the RM cloud on the window is possible, due to stimulated emission [33] and particle emission from the deposit. If the temperature becomes as low as in the time-of-flight studies in [19, 21], a solid state of RM at 20 K or lower can exist. This means that the reflection measurements sample a different phase of RM than the transmission experiments. Further studies, probably using a combination of

stimulated emission and Raman spectroscopy, are needed to give conclusive evidence in this case.

5.5 *Temperature changes of reflective window*

If the temperature of the ZnSe windows in the vacuum chamber changes, an influence on the reflection experiments from trivial reasons is very unlikely. Effects due to temperature changes could possibly be found due to changes in the refractive index of the windows, which may displace the laser beam slightly. However, the acceptance of the optics is large, and the opening diameter for the parallel laser beam is more than 20 mm through the FPI. Such temperature effects would be most obvious in the case of the reflection experiments, due to the larger angle towards the window normal in that case.

A case with heating of the reflective window in the chamber during a reflection experiment is shown in Fig. 6. The window was heated with a small drying fan to a temperature of 50–60 °C, and the resulting laser scan is shown together with a scan made before heating. In the experiments otherwise, the window is never heated more than a few degrees by the heat from the RM emitter. The interferometer fringes do not change in position but they increase in intensity, as described above. Thus, we conclude that the temperature of the window does not have any importance for the observed wavelength shifts.

6 Conclusions

It is concluded that low-intensity IR laser light shifts in wavelength during passage through Rydberg matter, giving both blue shifts and red shifts up to 0.02 cm^{-1} depending on the conditions of the Rydberg matter, especially its temperature and possibly also the state of the Rydberg matter, being liquid or crystalline. The mechanism giving the shifts is proposed to be stimulated Raman scattering. The shifts are observed with a temperature-stable Fabry–Pérot interferometer.

ACKNOWLEDGEMENTS The support from the Swedish Research Council for Engineering Sciences (TFR) and from the Swedish Research Council (VR) is gratefully acknowledged. One of the referees pointed out the possibility of a liquid–solid transition, which is also gratefully acknowledged.

REFERENCES

1 S. Badiei, L. Holmlid: Chem. Phys. Lett. **376**, 812 (2003)
2 L. Holmlid: J. Phys. B: At. Mol. Opt. Phys. **37**, 357 (2004)
3 S. Badiei, L. Holmlid: Phys. Lett. A **327**, 186 (2004)
4 V.S. Filinov, E.A. Manykin, B.B. Zelener, B.V. Zelener: Laser Phys. **14**, 186 (2004)
5 G.E. Norman: JETP Lett. **73**, 10 (2001)
6 S. Badiei, L. Holmlid: Mon. Not. R. Astron. Soc. **335**, L94 (2002)
7 L. Holmlid: Astrophys. Space Sci. **291**, 98 (2004)
8 L. Holmlid: Phys. Rev. A **63**, 013 817 (2001)
9 L. Holmlid: Eur. Phys. J. Appl. Phys. **26**, 103 (2004)
10 É.A. Manykin, M.I. Ozhovan, P.P. Poluéktov: Sov. Phys. Tech. Phys. Lett. **6**, 95 (1980)
11 É.A. Manykin, M.I. Ozhovan, P.P. Poluéktov: Sov. Phys. Dokl. **26**, 974 (1981)
12 R. Svensson, L. Holmlid, L. Lundgren: J. Appl. Phys. **70**, 1489 (1991)
13 R. Svensson, L. Holmlid: Surf. Sci. **269–270**, 695 (1992)
14 É.A. Manykin, M.I. Ozhovan, P.P. Poluéktov: Sov. Phys. JETP **75**, 440 (1992)
15 É.A. Manykin, M.I. Ozhovan, P.P. Poluéktov: Sov. Phys. JETP **75**, 602 (1992)
16 J. Wang, L. Holmlid: Chem. Phys. Lett. **295**, 500 (1998)
17 L. Holmlid: Chem. Phys. **237**, 11 (1998)
18 J. Wang, L. Holmlid: Chem. Phys. **261**, 481 (2000)
19 J. Wang, L. Holmlid: Chem. Phys. **277**, 201 (2002)
20 S. Badiei, L. Holmlid: Int. J. Mass Spectrom. **220**, 127 (2002)
21 S. Badiei, L. Holmlid: Chem. Phys. **282**, 137 (2002)
22 V.I. Yarygin, V.N. Sidelnikov, I.I. Kasikov, V.S. Mironov, S.M. Tulin: JETP Lett. **77**, 280 (2003)
23 A. Kotarba, J. Dmytrzyk, U. Narkiewicz, A. Baranski: React. Kinet. Catal. Lett. **74**, 143 (2001)
24 A. Kotarba, G. Adamski, Z. Sojka, S. Witkowski, G. Djega-Mariadassou: Stud. Surf. Sci. Catal. Part A **130**, 485 (2000)
25 A. Kotarba, A. Baranski, S. Hodorowicz, J. Sokolowski, A. Szytula, L. Holmlid: Catal. Lett. **67**, 129 (2000)
26 I.L. Beigman, V.S. Lebedev: Phys. Rep. **250**, 95 (1995)
27 L. Holmlid: J. Phys.: Condens. Matter **14**, 13 469 (2002)
28 R. Svensson, L. Holmlid: Phys. Rev. Lett. **83**, 1739 (1999)
29 J.C. White: in *Tunable Lasers* (Top. Appl. Phys. **59**), 2nd edn., ed. by L.F. Mollenauer, J.C. White, C.R. Pollock (Springer, Berlin 1992) p. 115
30 Y.R. Shen: *The Principles of Nonlinear Optics* (Wiley, New York 1984)
31 A. Yariv: *Quantum Electronics*, 3rd edn. (Wiley, New York 1989)
32 W. Demtröder: *Laser Spectroscopy, Basic Concepts and Instrumentation*, 2nd edn. (Springer, Berlin 1996)
33 L. Holmlid: Chem. Phys. Lett. **367**, 556 (2003)